Thermosensitive Soy Protein/Poly(*N*-isopropylacrylamide) Interpenetrating Polymer Network Hydrogels for Drug Controlled Release

Yong Liu,[1] Yingde Cui[2,3]

[1]*School of Chemistry and Chemical Engineering, Zhaoqing University, Zhaoqing, People's Republic of China*
[2]*Institute of Green Chemical Engineering, Zhongkai University of Agriculture and Engineering, Guangzhou, People's Republic of China*
[3]*School of Materials Science and Engineering, Northwestern Polytechnical University, Xi'an, People's Republic of China*

Received 22 July 2010; accepted 5 October 2010
DOI 10.1002/app.33535
Published online 14 February 2011 in Wiley Online Library (wileyonlinelibrary.com).

ABSTRACT: A series of the thermosensitive interpenetrating polymer network hydrogels composed of soy protein and poly(*N*-isopropylacrylamide) were successfully prepared. The structure and properties were systematically characterized by Fourier transform infrared spectroscopy, scanning electron microscopy, and differential scanning calorimetry. It was found that the hydrogels had good miscibility and high porosity, and the volume phase transition temperatures of the hydrogels were around 32°C. The release behavior and the release mechanism of a model protein, bovine serum albumin (BSA), were also investigated in detail. The results indicated that the release behavior of BSA had strong temperature dependence and the release percentage of BSA could be controlled by modulating the amount of soy protein or crosslinking agent. The analysis of the release mechanism revealed that the Fickian diffusion controlled release was dominant under the experimental conditions. © 2011 Wiley Periodicals, Inc. J Appl Polym Sci 120: 3613–3620, 2011

Key words: soy protein; poly(*N*-isopropylacrylamide); hydrogels; drug controlled release

INTRODUCTION

The stimuli-sensitive hydrogels, which are called "intelligent" or "smart" hydrogels, have been of significant interest in the design of drug delivery devices to modulate both the site and the release rate of drugs. Poly(*N*-isopropylacrylamide) (PNIPAAm), which shows a thermoreversible phase transition temperature of around 32°C, is a well-known thermosensitive polymer. Thus, the PNIPAAm-based hydrogels have been widely investigated and utilized in the field of drug delivery systems.[1]

In recent years, the natural polymers have attracted more and more interest in the development of new biomaterials and devices for the biomedical and pharmaceutical applications owing to the advantages of renewability, biodegradability, and low toxicity. To combine with the advantages of the natural polymers and PNIPAAm, PNIPAAm has been used to blend with some natural polymers, such as Kappa carrageenan,[2] guar gum,[3] chitosan,[4–8] cellulose,[9,10] alginate,[11–13] silk fibroin,[14,15] xanthan derivatives,[16] gelatin,[17] zein,[18] soybean oil,[19] to develop novel temperature-sensitive biomaterials for the biomedical utilization.

Over the past decade, systems based on the animal proteins including gelatin, collagen, casein, albumin, and whey protein have been studied for delivering drugs, nutrients, bioactive peptides, and probiotic organisms.[20] However, the plant proteins as the new devices for the biomedical utilization have not been fully investigated. Soy protein, an abundant renewable plant protein, may be regarded as an ideal biomaterial for biomedical, tissue engineering scaffold and drug delivery applications because of its good biodegradability and biocompatibility, readily availability, high thermal stability, and noncytotoxicity.[21–26] Recently, soy protein composites have been developed for cell cultures, drug carriers, and wound dressing materials.[20,21,27,28] Particularly, blending soy protein with environmentally sensitive polymers can endow the composites with intelligent features, which may result in new potential applications for the biomedical and pharmaceutical fields.[29,30] However, to the best of our knowledge, no investigation of thermosensitive soy protein/poly(*N*-isopropylacrylamide) interpenetrating polymer network (IPN) hydrogels for drug controlled release has been reported.

Correspondence to: Y. Cui (cuizku@gmail.com).
Contract grant sponsor: National Natural Science Foundation of China; contract grant number: 20776164.

Therefore, the purpose of this study was to prepare the soy protein/poly(*N*-isopropylacrylamide) IPN hydrogels and investigate the possibility of the hydrogels for drug controlled release. The structure and properties of the hydrogels were characterized, and the release behavior and release mechanism of a model protein, bovine serum albumin, from the hydrogels were also investigated in detail.

EXPERIMENTAL

Materials

Soy protein isolated (SPI) was from Dupont Yunmeng Protein (Hubei, China). *N*-isopropylacrylamide (NIPAAm) was bought from Tokyo Chemical Industry (Tokyo, Japan). Ammonium persulfate (APS, initiator) were obtained from Yongda Chemical Reagent (Tianjin, China). *N*,*N*′-methylenebisacrylamide (BIS, crosslinking agent for *N*-isopropylacrylamide) and glutaraldehyde (GA, crosslinking agent for SPI) were supplied by Kermel Chemical Reagent (Tianjin, China). Tetramethylethylenediamine (TEMED, accelerant) was purchased from Qianjin Chemical Reagent (Shanghai, China). Bovine serum albumin (BSA, model drug) was purchased from Shanghai Sinopharm Chemical Reagent (Shanghai, China). All the reagents were analytical grade.

Preparation of the hydrogels

Definite amount of NIPAAm was incorporated into the SPI solution to dissolve completely, and the volume of the mixture was adjusted to 15 mL by adding deionized water. Then continuously stirring and bubbling by nitrogen, the GA, BIS, APS, and TEMED were added into the mixture. Finally, this mixture was injected immediately into PVC tubes (6 mm diameter) to polymerize in a low temperature reactor of 15°C for 24 h. The hydrogels obtained were cut into pieces of 3 mm in length and immersed in deionized water to remove the unreacted residual reagents. The deionized water was refreshed every 4 h during this period. The swollen hydrogels were dried at room temperature and further dried at 40°C in a vacuum oven.

IR spectroscopy

Fourier transform infrared (FTIR) spectroscopy (Equinox 55, Bruker, Germany) was used to record the IR spectra of the dried NS0, NS2, SPI, BSA, and LNS2.

Morphology of the hydrogels

The hydrogels were swollen to equilibrium in deionized water and then were freeze-dried by the freeze dryer (LGJ-18, SHKY, China). The freeze-dried gels were coated with gold sputtering and the surface morphologies of the coated gels were examined by using scanning electron microscopy (SEM) (Quanta 400F, FEI, Netherlands) with an acceleration voltage of 20 kV.

Glass transition temperature of the hydrogels

The glass transition temperatures (T_g) of the dried hydrogels were investigated by differential scanning calorimetry (DSC 204, Netzsch, Germany). All samples were primarily heated from room temperature to 120°C at 20°C/min under a nitrogen atmosphere and then were cooled to room temperature. Second, the samples were reheated to 180°C at 10°C/min. The T_g of the dried hydrogels was determined from the second cycle where the midpoint of the inflection was taken as the T_g.

Volume phase transition temperature of the hydrogels

Volume phase transition temperature (VPTT) of the hydrogels was determined by DSC. The sample was swollen to equilibrium in deionized water at 25°C, and then about 10 mg of the sample was placed into a hermetic aluminum pan and sealed tightly with a hermetic aluminum lid. The sample was heated from 20 to 50°C at 2°C/min under a nitrogen atmosphere. The onset point of the endothermic peak was taken as the VPTT.

Drug loading and *in vitro* release

The model drug, bovine serum albumin (BSA), was loaded into the blank hydrogels by being immersed into the BSA aqueous solution (30 mg/mL) for 3 days at 4°C. The BSA-loaded hydrogels were first dried at room temperature for 3 days and further dried in a vacuum oven at 40°C to a constant weight. The BSA-loaded NS0, NS1, NS2, NS3, NS4, and NS5 were denoted as LNS0, LNS1, LNS2, LNS3, LNS4, and LNS5, respectively.

The dried BSA-loaded hydrogels were immersed in conical vials containing 30 mL of pH 7.4 buffer solution at various temperatures. The vials were closed and incubated in a thermostatic shaker (HY60, HCBioTch, China) with a speed of 60 rpm. At given time intervals, 3 mL of the solution was taken out to measure the amount of released BSA by UV–vis spectrophotometer (760CRT, Lengguang, China) at 280 nm, and then put back into the same vial. The released concentration was obtained from the calibration curve. The release percentage of the BSA from the loaded hydrogels was calculated by the following equation:

TABLE I
Feed Compositions and Samples of the Hydrogels

Samples	SPI (g)	GA (mL)	NIPAAm (g)	BIS (g)	APS (g)	TEMED (μL)
NS0	0.0	0.0	2.0	0.04	0.02	20
NS1	0.2	0.1	2.0	0.04	0.02	20
NS2	0.4	0.2	2.0	0.04	0.02	20
NS3	0.6	0.3	2.0	0.04	0.02	20
NS4	0.4	0.2	2.0	0.03	0.02	20
NS5	0.4	0.2	2.0	0.05	0.02	20

$$\textit{Cumulative release of BSA } (\%) = \frac{W_t}{W} \times 100 \qquad (1)$$

where W_t is the cumulative amount of BSA released at the time t and W is the initial amount of BSA loaded.

RESULTS AND DISCUSSION

Preparation of the IPN hydrogels

The soy protein/poly(*N*-isopropylacrylamide) IPN hydrogels were prepared by the simultaneous IPN method. To investigate the effect of soy protein content and crosslinking agent on the hydrogel properties, a series of samples was synthesized by free radical polymerization in aqueous solution using GA and BIS as the crosslinking agents and APS as the initiator. The hydrogels formed below the VPTT are homogeneous and have good mechanical properties, whereas those formed above the VPTT exhibit heterogeneous structures and have poor mechanical properties. It is known that the free radical polymerization reaction is exothermic. To avoid the heterogeneous structures and ensure the reaction temperature below the VPTT during the polymerization, the reaction was in a low temperature reactor of 15°C. The feed compositions and sample codes are shown in Table I.

Structure and morphology analysis

The FTIR spectra of NS0, NS2, SPI, BSA, and LNS2 are shown in Figure 1. As it is seen from the spectra of SPI and BSA, the main characteristic absorption bands at 3307 and 3306 cm^{-1} owing to the stretching vibration of *N*—H group are from SPI and BSA, respectively. The bands of SPI at 1658 and 1545 cm^{-1} are attributed to amide I (C=O) and Amide II (*N*—H), respectively, and those of BSA are at 1660 and 1534 cm^{-1}, respectively. In the spectra of NS0, NS2, and LNS2, the absorption bands at 3343, 3326, and 3329 cm^{-1} assigning to the stretching vibration of free *N*—H group are from NS0, NS2, and LNS2, respectively. The bands of Amide I at 1658, 1649, and 1649 cm^{-1} belong to NS0, NS2, and LNS2, respectively, while those of Amide II are at 1546, 1543, and 1542 cm^{-1}, respectively. In comparison to the spectra of SPI and NS0, the characteristic absorption bands of free *N*—H group, Amide I and Amide II in the spectrum of NS2 are shifted to 3326 cm^{-1}, 1649 and 1543 cm^{-1}, respectively. These characteristic absorption bands shifting to low wavenumber indicate that there are intermolecular hydrogen bonds between polymeric molecular chains of soy protein and poly(*N*-isopropylacrylamide).[15,31–33] Moreover, it is noticed that no new characteristic bands appear in the spectrum of NS2 except the characteristic bands shifting to low wavenumber, which verifies that the IPN structure is formed and there are intermolecular hydrogen bonds in hydrogel network.[29] In addition, compared with the spectra of BSA and NS2, no new characteristic bands appear in the spectrum of LNS2, which reveal that the absorption of BSA into the polymer matrix is the purely physical process.

The morphological images of the freeze-dried hydrogels (Fig. 2) show that all the hydrogels have porous, honey-like network structures, which were created with the formed ice crystals serving as pore-forming agents during the freezing step. It can be seen that these porous network structures have high porosity and interconnectivity, which will be good for the drug or water molecules in or out of the hydrogels. It is also observed that the content of SPI or BIS affects the regularity of the porous structures, which were caused by the different rate of gelation during the polymerization and crosslinking process.[15,34]

Differential scanning calorimetry analysis

Glass transition temperature (T_g) is one of the characteristic temperatures for the polymer blend. Measuring the T_g by DSC is a very effective way to

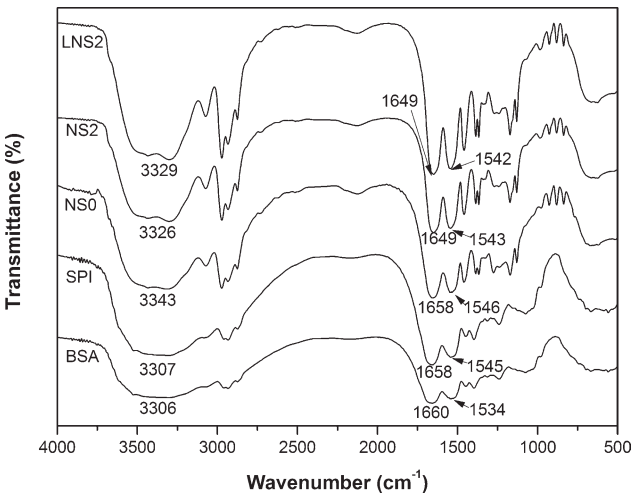

Figure 1 FTIR spectra of NS0, NS2, SPI, BSA, and LNS2.

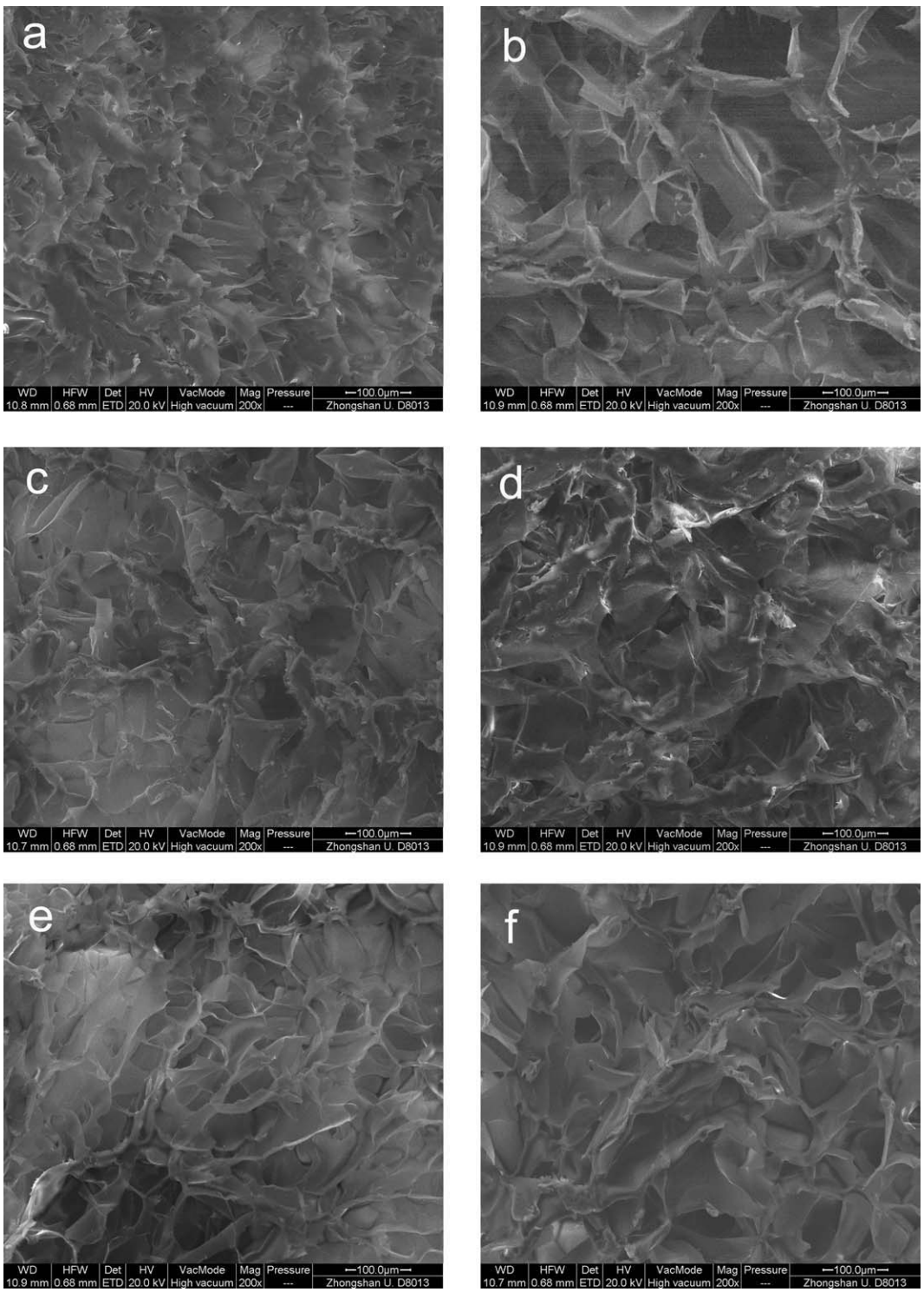

Figure 2 SEM micrographs of NS0 (a), NS1 (b), NS2 (c), NS3 (d), NS4 (e), and NS5 (f).

determine the miscibility of the polymer blend. The DSC thermograms of the dried hydrogels are depicted in Figure 3. It is clearly seen that a single T_g appears in all the samples, which suggests that the blend of poly(*N*-isopropylacrylamide) and SPI has good miscibility. The T_g of NS0, NS1, NS2, NS3, NS4, and NS5 is 123.6, 124.8, 125.3, 126.5, 124.6, and 127.1°C, respectively. The data demonstrate that the T_g gradually shifts to a high temperature with increasing the content of SPI or BIS. It may be attributed to the formation of the hydrogen bonds in the hydrogel network, which can retard the movement of polymer segments and will be the driving force for the miscibility of the polymer blend.[35] As a

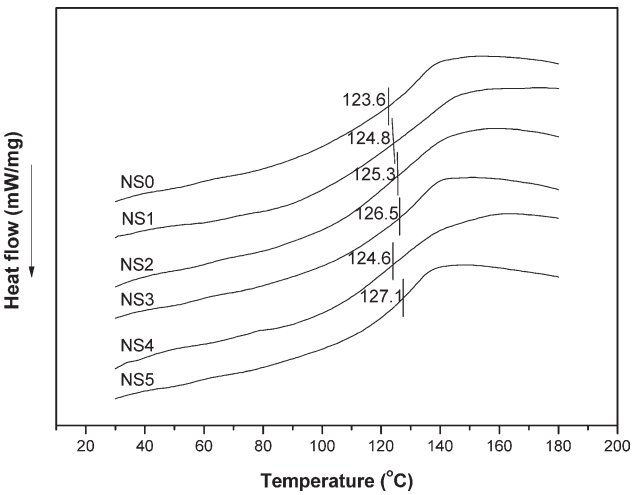

Figure 3 DSC thermograms of the dried hydrogels.

result, the higher the content of SPI or BIS, the higher T_g is obtained.

It is well known that PNIPAAm can undergo a hydrophilic/hydrophobic phase transition at a VPTT of about 32°C.[4,36] To measure the effect of SPI or BIS on the VPTT, the DSC was used to detect the VPTT. The DSC thermograms of the swollen hydrogels (Fig. 4) show that the VPTTs of NS0, NS1, NS2, NS3, NS4, and NS5 are 32.1, 32.5, 32.7, 32.7, 32.5, and 32.8°C, respectively. The VPTT behavior is resulted from the hydrophilic/hydrophobic balance in the hydrogel network, which can be affected by the hydrogen bonds. The data show that the content of SPI or BIS has a somewhat effect on the VPTT of the hydrogels.

Effect of temperature on BSA release

To evaluate the effect of temperature on BSA release, the dried hydrogel LNS2 was immersed

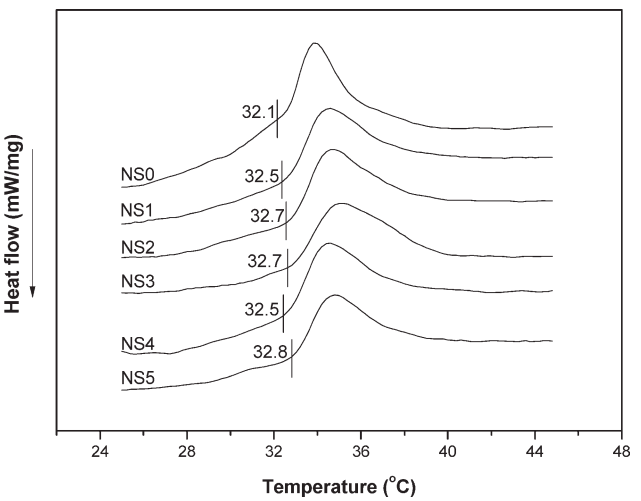

Figure 4 DSC thermograms of the swollen hydrogels.

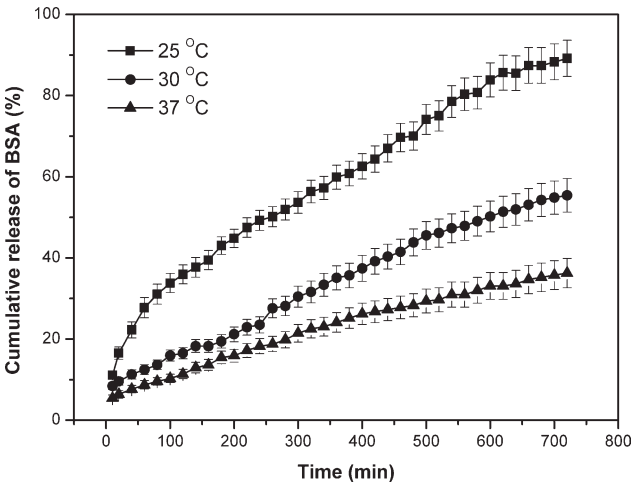

Figure 5 The dynamic release profiles of BSA from LNS2 in the buffer solution of pH 7.4 at various temperatures.

into the buffer solution of pH 7.4 at various temperatures to investigate the release behavior of BSA. The dynamic release profiles of BSA from LNS2 at various temperatures (Fig. 5) show that the release percentage of BSA decreases with increasing the temperature. It can be seen that the dynamic release curves of BSA are almost linear at 30 and 37°C, while the BSA release rate and the release amount at 25°C are higher than that of 30 and 37°C. In the hydrogel network, there is a hydrophilic/hydrophobic balance between the amide and isopropyl groups. When the temperature is below VPTT, the hydrogen bond action between the hydrophilic groups and water molecules is dominant, and the hydration structures, like a cage, around the hydrophobic group are formed. The hydration structures make the polymer chain in a state of stretching and relaxation, which can reduce the tortuous degree of channels and the diffusion resistance for BSA and consequently improve the release rate of BSA. Moreover, the hydration structures also make the water molecules more easily enter the polymer matrix and improve the movement of water molecules, which can enhance the dissolution of BSA within the hydrogels and improve the release rate of BSA. When the temperature is around or above VPTT, the hydrophobic effect of the hydrophobic groups becomes dominant and the hydration structures are destroyed, causing the intertwining of polymer chains and more compact structure in the hydrogel network. This compact structure can enhance the tortuous degree of channels and the diffusion resistance and reduce the movement of water molecules, which restrain the BSA release. All above information indicates that the release of BSA from the hydrogels has the strong temperature dependence.

Effect of soy protein content on BSA release

The dynamic release profiles of BSA from LNS0, LNS1, LNS2, and LNS3 in the buffer solution of pH 7.4 at 37°C are shown in Figure 6. It is clear in Figure 6 that the release percentage of BSA decreases with increasing the content of SPI. This can be explained by the fact that, as the content of SPI increase, the intermolecular physical entanglements and the role of hydrogen bonds increase in the hydrogel network, which reduce the relaxation and movement of the polymer chain and make the hydrogel networks tighter. This tight structure makes the water molecules diffuse into the hydrogels slower, resulting in the slower dissolution of BSA. At the same time, the tight structure also causes the increase of the diffusion resistance for BSA, which reduces the release percentage f BSA. Therefore, modulating the content of SPI can control the release percentage of BSA.

Effect of crosslinking agent content on BSA release

The dynamic release profiles of BSA from LNS2, LNS4, and LNS5 in the buffer solution of pH 7.4 at 37°C (Fig. 7) show that the release percentage of BSA decreases with increasing BIS content. This may be attributed to the main fact that the number of crosslink points increases in the polymer network by increasing the content of BIS, which lead to the smaller network mesh size, the reduction of voids available and the increase of physical entanglements of the polymer chains within the hydrogel network. As a result, increasing the content of BIS can restrain the relaxation of network chains and reduce the swelling ratio of the hydrogels, which make BSA inflexible towards diffusion and result in the decrease of BSA release. Therefore, the release of BSA can be controlled by modulating the content of BIS.

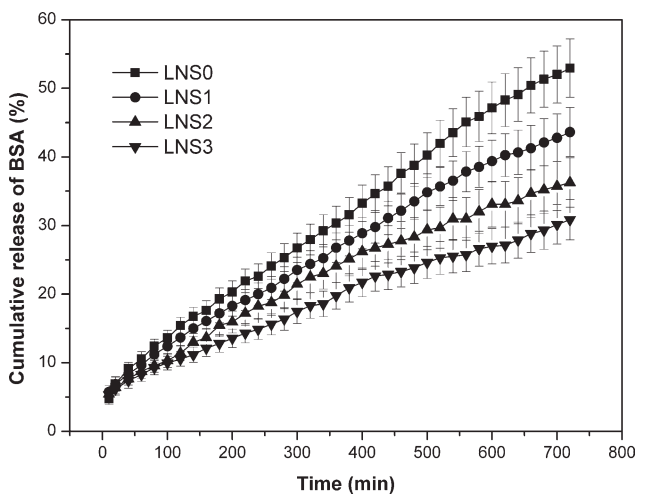

Figure 6 The dynamic release profiles of BSA from LNS0, LNS1, LNS2, and LNS3 in the buffer solution of pH 7.4 at 37°C.

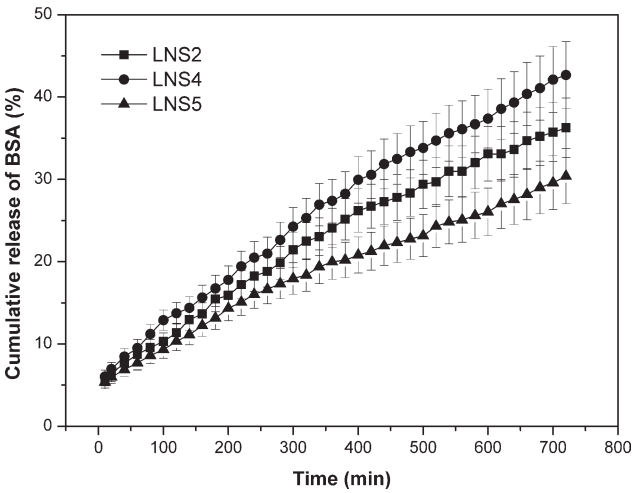

Figure 7 The dynamic release profiles of BSA from LNS2, LNS4, and LNS5 in the buffer solution of pH 7.4 at 37°C.

Evaluation of the release mechanism

To investigate the release mechanism of BSA from the IPN hydrogels, the release data were analyzed by using eq. (2) for $M_t/M_\infty < 0.6$ as follows[37–41]:

$$M_t/M_\infty = kt^n \tag{2}$$

Where M_t is the cumulative amount of BSA released at the time t. M_∞ is the total amount of BSA released, k is the release constant, and exponent n is the characteristic exponent related to the release mechanism of BSA. For cylinder, when $n = 0.45$, the release signifies Fickian diffusion; when $0.45 < n < 0.89$, the release indicates an anomalous transport; while $n = 0.89$, the mechanism is Case II transport, namely zero-order release. The exponent n can be obtained from the slope of the plot of $\ln(M_t/M_\infty)$ versus $\ln t$.

To explore the relationship between Fickian diffusional release and Case II transport, the release mechanism also was analyzed by eq. (3) as follows[40,42]:

$$\frac{M_t}{M_\infty} = k_1 t^m + k_2 t^{2m} \tag{3}$$

Where the first term of the right side is the Fickian contribution, and the second term is the Case II relationship contribution. The k_1 and k_2 are the Fickian and relaxation kinetic constant, respectively. The coefficient m is the Fickian diffusion exponent for a device of any geometrical shape exhibiting

TABLE II
Diffusional Exponents, Fickian, and Relaxational Constants for the Release of BSA from LNS2 in the Buffer Solution of pH 7.4 at Various Temperatures

	Equation (2)		Equation (3)		
Temperature (°C)	n	R^2	k_1 ($\text{min}^{-0.4375}$)	k_2 ($\text{min}^{-0.875}$)	R^2
25	0.50	0.99735	1.12932	0.096569	0.99819
30	0.44	0.95786	1.09514	0.042329	0.99969
37	0.45	0.96526	0.99847	0.039620	0.99868

controlled release and is dependent of the aspect ratio of the device.

The diffusional exponents, Fickian and relaxational constants for the release of BSA obtained from fitting the eqs. (2) and (3) are shown in Tables II and III. As it is seen from Tables II and III, the values of n for the release of BSA from LNS2 at 25, 30, and 37°C are 0.50, 0.44, and 0.45, respectively, while the values of n for LNS0, LNS1, LNS2, LNS3, LNS4, and LNS5 at 37°C are 0.51, 0.48, 0.45, 0.40, 0.49, and 0.43, respectively. These results indicate that the release of BSA at the temperature around or above VPTT belongs to Fickian diffusion controlled release, and that of the temperature below VPTT signifies anomalous transport. Moreover, the higher the content of SPI or BIS, the lower is the value of n. According to the data, we can also see that the values of n for LNS0, LNS1, and LNS4 are slightly higher than 0.45, indicating that the Fickian diffusion controlled release is dominant. It is also observed that the Fickian kinetic constants (k_1) are greater than the relaxation kinetic constants (k_2), further confirming that the release mainly followed Fickian diffusion controlled release.

To estimate the percentage of relaxation and Fickian drug release, the ratio of relaxation (R) over Fickian (F) contributions was calculated by using eq. (4) as follows[42]:

$$\frac{R}{F} = \frac{k_2}{k_1} t^m \tag{4}$$

TABLE III
Diffusional Exponents, Fickian, and Relaxational Constants for the Release of BSA from Samples in the Buffer Solution of pH 7.4 at 37°C

	Equation (2)		Equation (3)		
Samples	n	R^2	K_1 ($\text{min}^{-0.4375}$)	k_2 ($\text{min}^{-0.875}$)	R^2
LNS0	0.51	0.98379	0.98105	0.07370	0.99916
LNS1	0.48	0.97728	1.07246	0.05573	0.99925
LNS2	0.45	0.96526	0.99847	0.039620	0.99868
LNS3	0.40	0.95739	0.99417	0.030307	0.99909
LNS4	0.49	0.96738	1.13335	0.071491	0.99929
LNS5	0.43	0.96288	1.06464	0.033322	0.99913

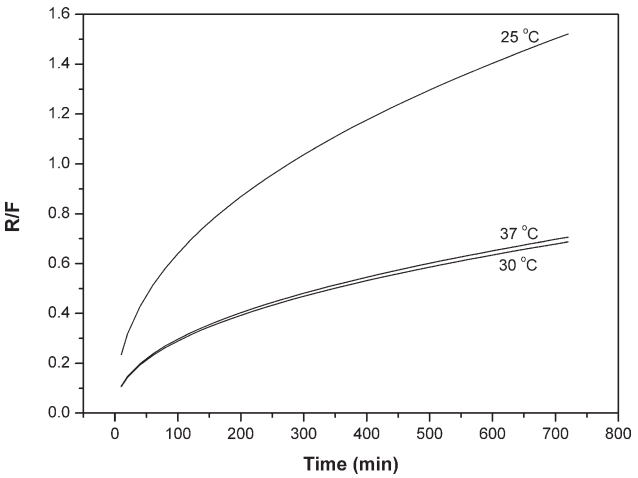

Figure 8 R/F ratio as a function of release time in LNS2 at various temperatures.

The results of the ratio R/F versus t are plotted in Figures 8 and 9. It is noticed in Figure 8 that the ratio R/F at 25°C is larger than that of 30 and 37°C, and the ratio R/F at 25°C is more than 1.0 in most of the time whereas that of 30 and 37°C is always less than 1.0, which indicates that the relaxation contributions are dominant at 25°C but Fickian contributions predominate at 30 and 37°C. In Figure 9, the ratio R/F decreases with the increase of SPI or BIS, and the ratio R/F is almost less than 1.0, indicating that the Fickian diffusion contributions predominate at 37°C and gradually increase with increasing the amount of SPI or BIS. Therefore, the temperature plays an important role in controlling the release of BSA, and SPI or BIS also has an important effect on the release mechanism. We also can see that Fickian contributions of the release from LNS1, LNS2, LNS3, and LNS5 at 30 and 37°C are over relaxation contributions, while relaxation contributions of the release from LNS0, LNS4 at 37°C and LNS2 at 25°C

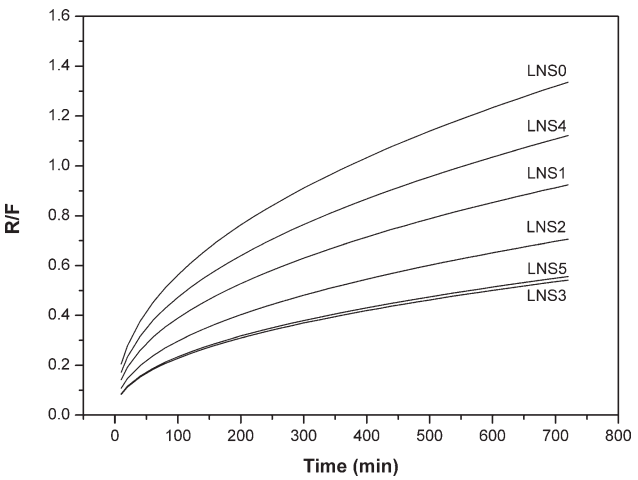

Figure 9 R/F ratio as a function of release time in all samples at 37°C.

gradually become predominant role after 360, 540, and 260 min, respectively.

CONCLUSIONS

In this work, the thermosensitive soy protein/poly(*N*-isopropylacrylamide) IPN hydrogels have been prepared by free radical polymerization in the presence of GA and BIS as the crosslinking agents and APS as the initiator. The intermolecular hydrogen bonds between polymeric molecular chains of soy protein and poly(*N*-isopropylacrylamide) have been confirmed by FTIR. The higher content of soy protein, the stronger intermolecular hydrogen bonds are obtained. The VPTTs of the hydrogels are around 32°C, and the IPN hydrogels have good miscibility and high porosity and interconnectivity. The release of BSA from the hydrogels has strong temperature dependence, and controlling the content of SPI or BIS can modulate the release percentage of BSA. The release mechanism of BSA is dominantly the Fickian diffusion controlled release under the experimental conditions. The tunable properties of these IPN hydrogels are promising candidates to be served as thermosensitive drug delivery systems.

References

1. Milaîsinović, N.; Kruîsić, M. K.; Kneîzević-Jugović, Z.; Filipović, J. Int J Pharm 2010, 383, 53.
2. Zhai, M. L.; Zhang, Y. Q.; Ren, J.; Yi, M.; Ha, H. F.; Kennedy, J. F. Carbohyd Polym 2004, 58, 35.
3. Li, X. Y.; Wu, W. H.; Liu, W. Q. Carbohyd Polym 2008, 71, 394.
4. Zhang, H. F.; Zhong, H.; Zhang, L. L.; Chen, S. B.; Zhao, Y. J.; Zhu, Y. L. Carbohyd Polym 2009, 77, 785.
5. Don, T. M.; Chen, H. R. Carbohyd Polym 2005, 61, 334.
6. Cao, Y.; Zhang, C.; Shen, W.; Cheng, Z.; Yu, L.; Ping, Q. J Control Release 2007, 120, 186.
7. Chen, X.; Song, H.; Fang, T.; Bai, J.; Xiong, J.; Ying, H. J Appl Polym Sci 2010, 116, 1342.
8. Verestiuc, L.; Ivanov, C.; Barbu, E.; Tsibouklis, J. Int J Pharm 2004, 269, 185.
9. Hao, Y.; Peng, J.; Li, J. Q.; Zhai, M. L.; Wei, G. S. Carbohyd Polym 2009, 77, 779.
10. Ifuku, S.; Kadla, J. F. Biomacromolecules 2008, 9, 3308.
11. Reddy, K. M.; Babu, V. R.; Rao, K. S. V. K.; Subha, M. C. S.; Rao, K. C.; Sairam, M.; Aminabhavi, T. M. J Appl Polym Sci 2008, 107, 2820.
12. Shi, J.; Alves, N. M.; Mano, J. F. Macromol Biosci 2006, 6, 358.
13. Zhang, G. Q.; Zha, L. S.; Zhou, M. H.; Ma, J. H.; Liang, B. R. J Appl Polym Sci 1931, 2005, 97.
14. Gil, E. S.; Hudson, S. M. Biomacromolecules 2007, 8, 258.
15. Wu, W.; Li, W.; Wang, L. Q.; Tu, K.; Sun, W. Polym Int 2006, 55, 513.
16. Hamcerencu, M.; Desbrieres, J.; Popa, M.; Riess, G. Biomacromolecules 1911, 10, 2009.
17. Dhara, D.; Rathna, G. V. N.; Chatterji, P. R. Langmuir 2000, 16, 2424.
18. Bromberg, L. J Phys Chem B 1997, 101, 504.
19. Alli, A.; Hazer, B. Eur Polym Mater 2008, 44, 1701.
20. Chen, L. Y.; Remondetto, G.; Rouabhia, M.; Subirade, M. Biomaterials 2008, 29, 3750.
21. Vaz, C. M.; van-Doeveren, P. F. N. M.; Reis, R. L.; Cunha, A. M. Polymer 2003, 44, 5983.
22. Kumar, R.; Choudhary, V.; Mishra, S.; Varma, I. K.; Mattiason, B. Ind Crop Prod 2002, 16, 155.
23. Vaz, C. M.; van-Doeveren, P. F. N. M.; Yilmaz, G.; de-Graaf, L. A.; Reis, R. L.; Cunha, A. M. J Appl Polym Sci 2005, 97, 604.
24. Silva, G. A.; Vaz, C. M.; Coutinho, O. P.; Cunha, A. M.; Reis, R. L. J Mater Sci: Mater Med 2003, 14, 1055.
25. Liu, D. G.; Tian, H. F.; Jia, X. W.; Zhang, L. N. Macromol Biosci 2008, 8, 401.
26. Zheng, H.; Zhou, Z. Y.; Chen, Y.; Huang, J.; Xiong, F. L. J Appl Polym Sci 2007, 106, 1034.
27. Snyders, R.; Shingel, K. I.; Zabeida, O.; Roberge, C.; Faure, M. P.; Martinu, L. J Biomed Mater Res A 2007, 83, 88.
28. Vaz, C. M.; De-Graaf, L. A.; Reis, R. L.; Cunha, A. M. Mater Res Innov 2004, 8, 149.
29. Liu, Y.; Cui, Y. D.; Yin, G. Q.; Luo, L. Z. J Biobased Mater Bioenergy 2009, 3, 437.
30. Liu, Y.; Cui, Y. D.; Yin, G. Q.; Ma, H. C. Iran Polym J 2009, 18, 339.
31. Chen, Y.; Zhang, L.; Gu, J.; Liu, J. J Membr Sci 2004, 241, 393.
32. Silva, S. S.; Goodfellow, B. J.; Benesch, J.; Rocha, J.; Mano, J. F.; Reis, R. L. Carbohyd Polym 2007, 70, 25.
33. Wang, Q.; Du, Y.; Hu, X.; Yang, J.; Fan, L.; Feng, T. J Appl Polym Sci 2006, 101, 425.
34. Yang, J.; Winnik, M. A. Macromolecules 1996, 29, 7055.
35. Jin, S.; Liu, M.; Zhang, F.; Chen, S.; Niu, A. Polymer 2006, 47, 1526.
36. Brazel, C. S.; Peppas, N. A. Macromolecules 1995, 28, 8016.
37. Ritger, P. L.; Peppas, N. A. J Controlled Release 1987, 5, 37.
38. Lee, K. Y.; Park, W. H.; Ha, W. S. J Appl Polym Sci 1997, 63, 425.
39. Sakiyama, T.; Takata, H.; Kikuchi, M.; Nakanishi, K. J Appl Polym Sci 1999, 73, 2227.
40. Lara, M. G.; Bentley, M. V. O. L. B.; Collett, J. H. Int J Pharm 2005, 293, 241.
41. Bajpai, S.; Dubey, S. Polym Int 2004, 53, 2178.
42. Peppas, N. A.; Sahlin, J. J. Int J Pharm 1989, 57, 169.